Konrad Ziemianin

Oil and Gas Institute – National Research Institute

Anna Wolska

Institute of Geological Sciences, Jagiellonian University

Mineralogical and petrological characteristics of exotic schist cobbles from the Krosno Beds (Silesian Unit, Bieszczady Mts., south-east Poland)

Exotic schist cobbles were collected from two localities: Roztoki Dolne and Ustrzyki Górne (Krosno Beds, Silesian Nappe, Bieszczady Mts., SE Poland), where they occur in streams as a detrital material. These cobbles reach up to 25 cm in diameter, but a few boulders (up to 1 m) were also found. They were grey and green in colour and had mica and quartz layers (most often thicker than 0.5 cm, although some quartz layers can reach 1 cm). Some exotic cobbles found were tectonically deformed. These investigated schist cobbles consisted of quartz, white mica (phengite) and chlorite. Additionally other minerals which also occurred in cobbles were: garnet (almandine), tourmaline (dravite), and accessory: apatite, zircon, rutile and ilmenite. Biotite (often altered) and feldspar (albite, oligoclase) are rare. Numerous calcite veins were observed. Garnet porphyroblasts had different shapes (spherical, elliptic or tectonically elongated) and sometimes showed zonation. Tourmalines had characteristic blue and brown zones, due to variable contents of Fe. The protolith of the schists analyzed had the character of pelitic-mudstone rocks. The precursor rocks were metamorphosed during both progressive (almandine-amphibolite facies) and retrogressive metamorphism. The north-west extension of the Marmarosh or Rakhiv massifs between Dukla and Silesian subbasins was the most probable source of these exotic cobbles.

Key words: Bieszczady Mts., Krosno Beds, exotic cobbles, schist, garnet porphyroblast, tourmaline.

Charakterystyka mineralogiczno-petrologiczna łupków egzotykowych z warstw krośnieńskich (jednostka śląska, Bieszczady, płd.-wsch. Polska)

Łupki egzotykowe zostały pobrane z dwóch lokalizacji: Roztoki Dolne i Ustrzyki Górne (warstwy krośnieńskie, jednostka śląska, Bieszczady, południowo-wschodnia Polska), gdzie występowały jako materiał detrytyczny w korytach potoków. Ich wielkość na ogół nie przekracza 25 cm, aczkolwiek zanotowano również kilka większych okruchów (do 1 m średnicy). Charakteryzują się kolorem szaro-zielonym, z laminami mik i kwarcu dochodzącymi do 1 cm grubości, aczkolwiek najczęściej nie przekraczającymi 0,5 cm. Część z odnalezionych okazów wykazuje cechy tektonicznej deformacji. Zbadane łupki zbudowane są z kwarcu, jasnej miki (fengit) oraz chlorytu. Dodatkowo obserwuje się granat (almandyn), turmalin (drawit), a także akcesorycznie apatyt, cyrkon, rutyl oraz ilmenit. Biotyt (często przeobrażony) oraz skalenie (albit, oligoklaz) są rzadkie. Notuje się liczne żyły kalcytowe. Porfiroblasty granatu charakteryzują się zmiennym kształtem – od okrągłych, przez eliptyczne do tektonicznie wydłużonych. Niekiedy występuje u nich zonacja. Turmaliny posiadają charakterystyczną niebiesko-brązową zonację, wynikającą z różnej zawartości Fe. Protolit analizowanych łupków miał charakter pelityczno-mułowcowy. Uległ on metamorfizmowi zarówno progresywnemu w warunkach facji almandynowo-amfibolitowej, jak również retrogresywnemu. Północno-zachodnie przedłużenie masywu Marmarowskiego lub Rachowskiego (pomiędzy basenami śląskim i dukielskim) jest najbardziej prawdopodobnym obszarem źródłowym analizowanych skał egzotykowych.

Słowa kluczowe: Bieszczady, warstwy krośnieńskie, łupki egzotykowe, granat, turmalin.

Introduction

The aim of the works (which is still relatively incomplete) on the exotic rocks [11, 15] is to provide information about the basement of the Carpathians. It is necessary to understand the complicated history of the Carpathian region, as it plays the key role in the petroleum industry [13, 17].

The area studied is located in the Bieszczady Mts. (SE Poland) in the southern part of the Silesian Nappe – called the Central Carpathian Depression. In the border zone of this area there are distinguished systems of faults and flakes which connect with overthrust of the Dukla Nappe [18, 22–25]. In this zone flysch deposits are strongly deformed tectonically. There are deposits of deep-marine sediments, thick- and thin-bedded coarse-grained sandstone and shale. The total thickness of Silesian Nappe deposits reaches 2000 m [25]. In Krosno Beds, several exotic-bearing layers were found and described in numerous outcrops: Ustrzyki Górne [14], Roztoki Dolne and Baligród [19, 21], Bukowiec [20], Opołonek Mt and Połonina Wetlińska Mt [7], Wetlina–Owczarnia stream, Osada stream [3].

Geological setting

The described exotic cobbles of metamorphic rocks from the Krosno Beds were found in two outcrops: Roztoki Dolne (Mchawka stream) and Ustrzyki Górne (Zakopianiec stream). Both outcrops of exotic-bearing layers occur in synclines developed from the Krosno Beds (Lower). The Roztoki Dolne Syncline is a continuation to north-western extension (direction) of the Ustrzyki Górne Syncline [25]. The Krosno Beds (Oligocene) are represented here by argillaceous, calcareous sandstones and dark grey sandy shales with thick-bedded Otryt sandstone packages [21, 25] and their thickness reaches one hundred metres. These deposits include olistostromal sediments (melanges) – exotic pebbles, cobbles and boulders of metamorphic rocks (schists, amphibolites, gneisses) and microfauna limestones (Upper Eocene). Exotic cobbles derived as basement rocks from the Marmarosh or Rakhiv massifs [4, 13, 19, 21].

Two exotic-bearing layers (horizons) – lower (ca. 50 cm thick) and higher (ca. 2 m thick) in the northern limb of the Roztoki Dolne Syncline (Fig. 1) – were described [19]. The outcrop of layers with exotic cobbles in Roztoki Dolne (Mchawka stream) is located in a so called "transition zone" between thin-bedded sandstone and thick-bedded sandstone and shale of the lower division of the Krosno Beds [19, 21].

The outcrop of the exotic-bearing layer in Ustrzyki Górne area (affluent of the Zakopianiec stream) is located in the axial part of the Ustrzyki Górne Syncline [25] or the Brzeżna Syncline [12]. The N-E limb of the Ustrzyki Górne (Brzeżna) Syncline is formed from thick bedded Otryt sandstone packages belonging to the middle division of the Lower Krosno Beds. The exotic-bearing layers were described [25] as horizons located about c.a. 250 m higher from the top of the youngest Otryt sandstone packages (Fig. 2).

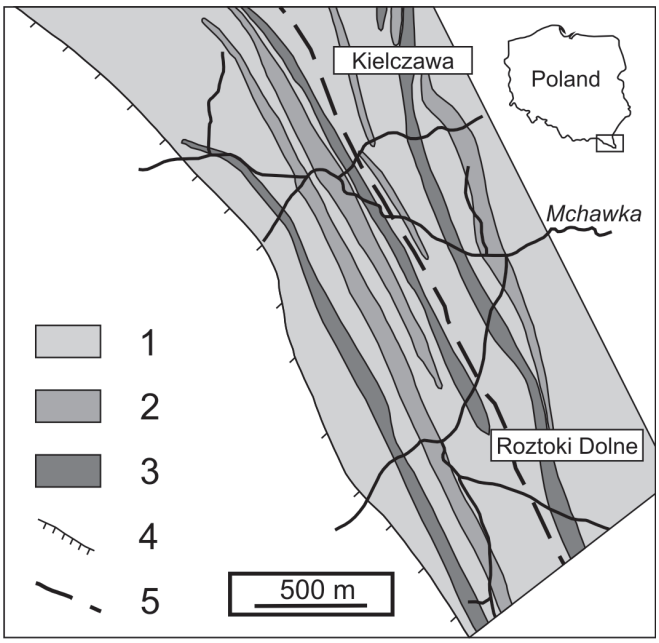

Fig. 1. Geological map of the Roztoki Dolne syncline [21]

1 – shales and sandstones, 2 – exotic-bearing layers, 3 – thick-bedded Otryt sandstones, 4 – overthrust of the Kalanica, 5 – syncline axis

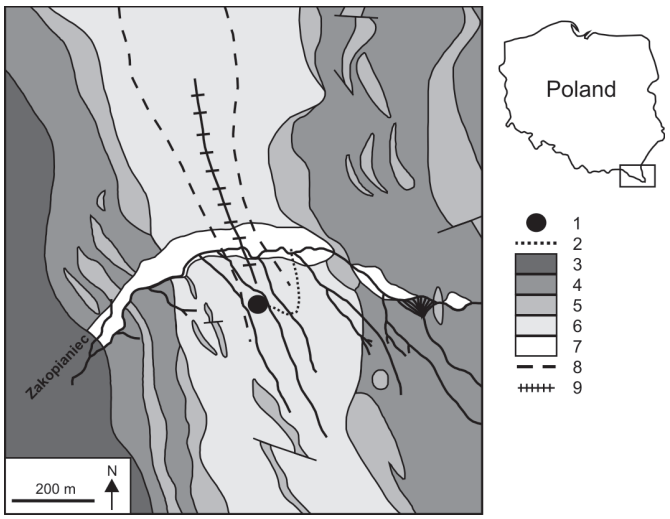

Fig. 2. Geological map of the Ustrzyki Górne area [14]

1 – the main outcrop where exotic rocks were found, 2 – border line of exotic rocks occurrence, 3 – Fore-Dukla zone, 4 – thin-bedded flysch deposits of the middle division of lower Krosno Beds, 5 – the Otryt sandstones, 6 – thin-bedded flysch deposits of the upper division of lower Krosno Beds, 7 – Quaternary deposits, 8 – syncline axis, 9 – anticline axis

Methods

Field work

Field trips were aimed at finding as many exotic rock pebbles and cobbles as possible to get enough samples for further analyses. During these trips special attention was paid to detrital material in alluvias. The authors also attempted to find exotic-bearing layers and get exotic rocks *in situ*.

Many exotic schist cobbles were found near Ustrzyki Górne. They were found in two subsequent affluents of Zakopianiec stream, where they occurred as a detrital material in alluvias at a distance of 30 m. The average size of the exotic rock cobbles found there was 15 × 10 × 5 cm, although a larger boulder (30 × 20 × 15 cm) was also observed.

The authors also found exotic schist cobbles near Roztoki Dolne. Lots of cobbles of exotic rocks were found in the Mchawka stream. Exotic schist cobbles from this locality also occurred as a detrital material in alluvias. The average size of the exotic schist cobbles was similar to the size of those noticed in Ustrzyki Górne, although one block of exotic schist that reached about 120 × 80 × 70 cm was found.

Macroscopic and microscopic investigations

The colour, foliation, presence of garnets (or its lack) and character of tectonic deformations for 16 samples of exotic schist cobbles was described. The results were useful for the classification of the samples into different groups and choosing the most representative and interesting samples for further studies.

The aim of microscopic observations (performed on thin sections with the use of Nikon Eclipse E600 Pol microscope, magnifications 20÷500x) was to identify and describe rock-formation and accessory minerals. In order to define the percentage values of those minerals, modal analysis was done. Thin sections were cut perpendicular to the foliation. Microphotographic documentation was done using a Nikon digital camera.

Cathodoluminescence

Cathodoluminescence investigations were done using a cold cathode CITL 8200 Mk 3a mounted on Nikon Eclipse E600 Pol. Average voltage was 600÷900 mA, while beam currents were 16÷19 kV.

SEM-EDS analysis

The chemical composition of minerals was determined using the SEM-EDS method. Universal thin sections of selected samples were analyzed using a field emission scanning microscope, Hitachi S-4700, equipped with an energy dispersive spectrometer, NORAN Voyager 3100. Time of analysis was 100 s for a point, accelerating current 20 kV. The ZAF correction algorithm was used.

Results

All collected exotic schist cobbles have a generally grey-greenish color. However, this color is not the same for every sample and it varies from pale grey, through grey (often with a brown shade) to grey-green (Fig. 3A, B).

Cobbles of investigated schists have an ellipsoidal or a rod shape. These shapes are as a result of fracturing along the foliation surfaces during transport. Size, position and relations between mica and quartz layers are different in each sample of investigated schist cobbles, which often change even within the same specimen.

Mica and quartz layers are most often up to 2 mm thick and occur alternately in a regular way (Fig. 3A). Sometimes large quartz layers (about 1 cm thick) can be noticed.

Mica layers can also be very thin (about 1 mm thick) and occur in thicker packages. Those packages can occur alternately with quartz layers that sometimes have the same thickness.

Mica layers can also be irregular. In such a situation quartz layers are noticeably larger (0.5÷1 cm) and also irregular (Fig. 3B).

In many samples red garnet porphyroblasts can be noticed. Their size rangess from 1 mm to 5÷6 mm. Although they are usually spherical or oval, some of them are tectonically elongated.

In some samples strong tectonic deformations and larger quartz layers (1 cm or even thicker) can be observed.

Schistose structure (observed with well developed mica-chlorite and quartz layers) is clearly visible in optical microscopic study. Mica-chlorite layers can occur in larger lamines and create s-c structures (mica fish). There are characteristic porphyroblasts of garnets and plagioclases noticed in the investigated exotic schists. In the case of garnet porphyroblasts, in their pressure shadows the growth of quartz is observed (Fig. 3D).

For all collected samples modal analysis was done (Tab. 1).

Quartz

In investigated schist cobbles, quartz is the main rock-forming mineral (37.9÷77.4 vol. %). It reaches up to 0.4 mm

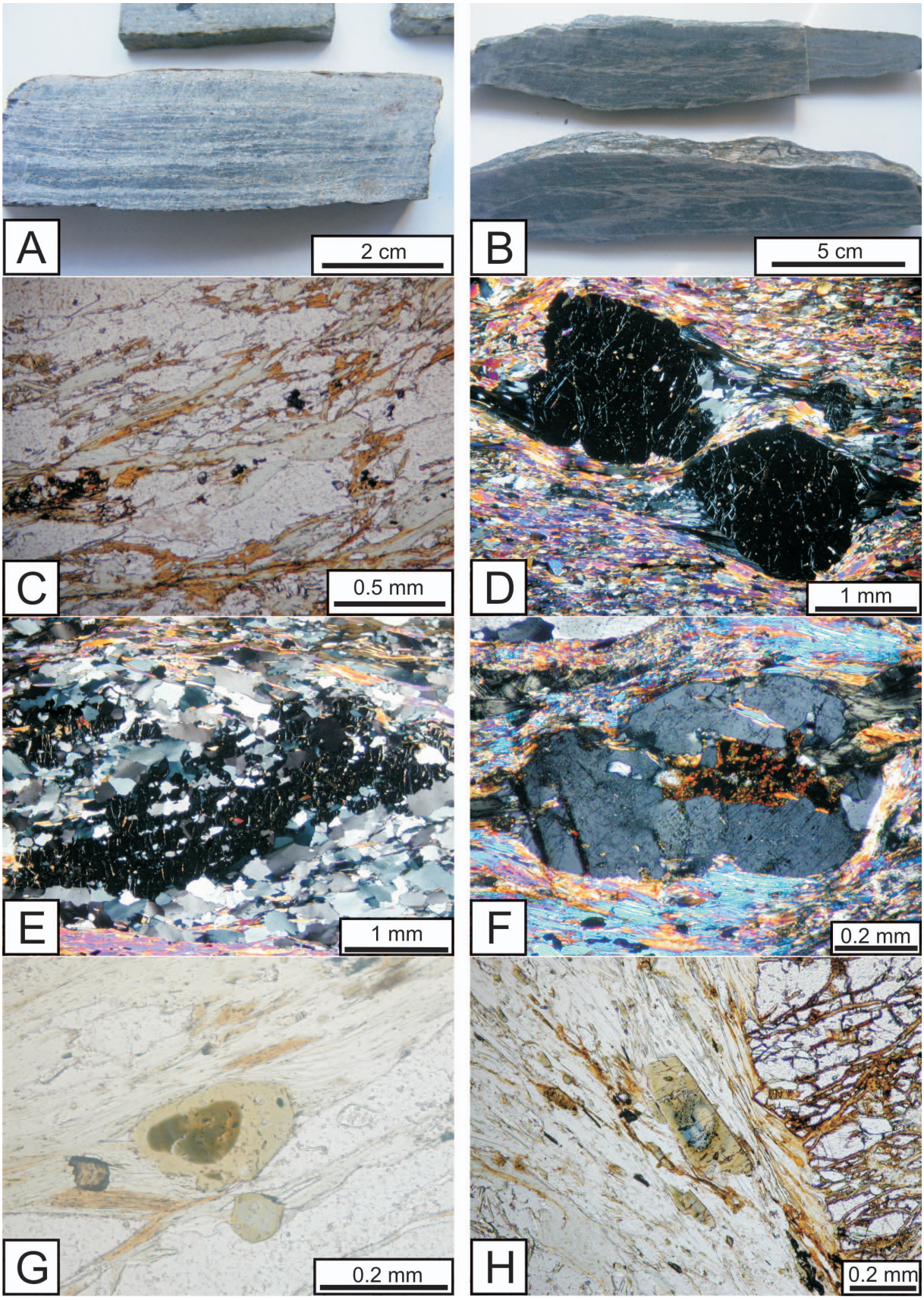

Fig. 3. Photographs and microphotographs of collected exotic schists cobbles

A – sample b.1.4 with regular, thin mica and quartz lamines and garnet porphyroblasts; B – sample a.4, irregular thin mica layers and larger quartz layers; C – sample a.3, chlorotization of biotite, relics with characteristic brownish pleochroism are well presented; D – sample a.1, garnet porphyroblasts with quartz grown in pressure shadows, crossed polars; E – sample b.1.4, tectonically elongated garnet porphyroblast, crossed polars; F – sample a.3, feldspar porphyroblast, crossed polars; G – sample b.1.1, a tourmaline with a very intense brown zone; H – sample a.2, a tourmaline with a blue zone.

Table 1. Modal analysis [vol. %]

Sample	Mineral composition [vol. %]										
	Quartz	Muscovite	Biotite	Chlorite	Garnet	Tourmaline	Apatite	Zirkon	Opaque minerals	Feldspar	Calcite
A.1	37.9	42.5	0.9	9.1	7.7	0.3	0.3	0	1.3	0.1	0
A.2	50.8	28.0	3.5	5.9	8.7	1.1	0.5	0.1	1.5	0	0
A.3	77.4	5.7	8.0	5.1	0	0	1.8	0	0.6	1.3	0
A.4	75.9	11.1	6.4	3.8	0	1.6	0.5	0	0.4	0	0.3
B.1.1	58,0	22.2	2.4	9.9	4.4	1.2	0.6	0.3	0.6	0.5	0
B.1.2	54.1	28.3	5.5	8.8	0.9	0.9	0.5	0.1	0.5	0.4	0
B.1.4	55.1	29.3	1.1	10.5	0.2	2.5	0.5	0.1	0.5	0.3	0
B.2.1	57.4	23.9	3.2	4.2	0	1.1	0.6	0	0.5	6.0	3.2

in size. Blasts of quartz form monomineral layers, but can also be noticed in mica-chlorite layers, in pressure shadows of garnet porphyroblasts or as inclusions in garnets. Quartz blasts show characteristic undulatory extinction, which suggests deformation of its structure.

White mica

White mica, which is the second main mineral in the investigated samples, reaches 22.2÷42.5 vol. %. White mica most often forms larger laminae with chlorite, although it can occur as a monomineral layer. Sometimes it can also fill fractures in garnet porphyroblasts.

Chemical analysis (SEM-EDS) of white mica revealed that they consist of 2.18÷3.64 wt. % Fe_2O_3 and 1.44÷1.99 wt. % MgO (the sum of Fe and Mg is 0.482÷0.677). The Si/Al^{IV} ratio ranges from 3.111 to 4.128. This high Si/Al^{IV} ratio in tetrahedral site and Fe and Mg partly replacing Al^{VI} in octahedral site may suggest that analyzed white micas are phengites. According to Borkowska and Smulikowski [5] phengite is a variety of muscovite, with the Si/Al^{IV} ratio higher than 3. All the analyzed white micas meet this requirement. Points representing the SEM-EDS analysis of white mica were plotted on the M^{2+}-Al-Si diagram (Fig. 4). They are found between the muscovite and phengite fields, which seem to confirm previous conclusions.

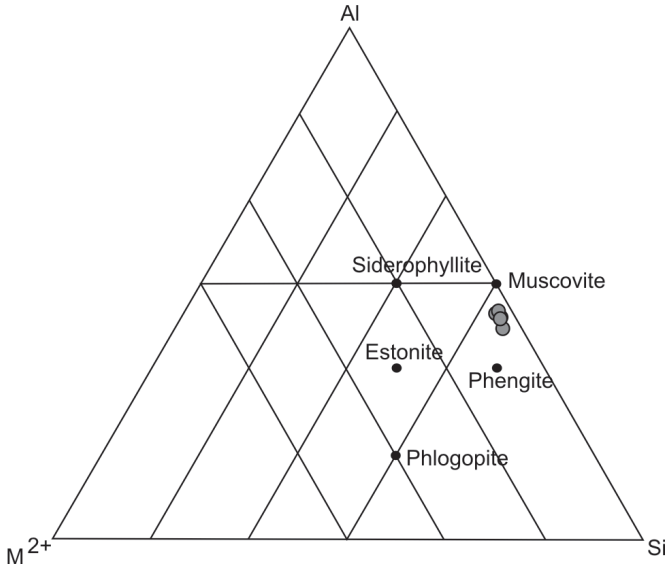

Fig. 4. M^{2+}-Al-Si diagram of mica-group composition

Biotite

Besides white mica, biotite is also present in investigated rocks. It reaches 0.9÷8 vol. %. The relatively low quantity of this mineral in all rock samples is a result of advanced chloritization process. Biotite rarely creates monomineral layers. Most often it can be perceived as single pseudohexagonal plates with only a few relics where characteristic brownish pleochroism is preserved. SEM-EDS analysis revealed a lower amount of K_2O (4.03÷5.00 wt. %) compared to a chemical composition of unaltered biotite. This amount of K_2O is a result of chloritization process. It seems to be more appropriate to name those dark micas as hydrobiotites or some phases between biotite and chlorite.

Chlorite

Chlorite, which is a product of biotite alternation (Fig. 3C), reaches 3.8÷10.5 vol. %. in investigated rock samples. It occurs in monomineral laminae or in mica-chlorite laminae. It can also be perceived as inclusion in garnet porphyroblasts. Classification of chlorites in investigated rocks is not easy due to the lack of ability to measure values of both Fe^{2+} and Fe^{3+} during SEM-EDS analysis. Because of that, points representing chemical analysis of chlorites, plotted in Hey's diagram (Fig. 5) can only be interpreted as an approximation. Chlorites chosen for the SEM-EDS analysis occur both in lamines and garnet porphyroblasts.

Most points representing chemical analysis of chlorites from chlorite-mica laminae are plotted on Hey's diagram in the ripidolite area. Only a few points are plotted in brunsvigite

or pycnochlorite fields. On the basis of SEM-EDS analysis results, two different types of chlorites in chlorite-mica laminae were noticed. These types have different magnesium numbers and are plotted in different positions on Hey's diagram – chlorites with a higher magnesium number (#mg = 0.526÷0.589) are lower within the ripidolite area, while those with a lower magnesium number (#mg = 0.319÷0.418) are higher within the ripidolite area.

Quite a similar position as chlorites from laminae (especially those with lower #mg) have chlorites from garnet porphyroblasts. The only difference is that chlorites from garnets porphyroblasts are a little higher within the described fields due to higher value of Fe (#mg = 0.203÷0.263).

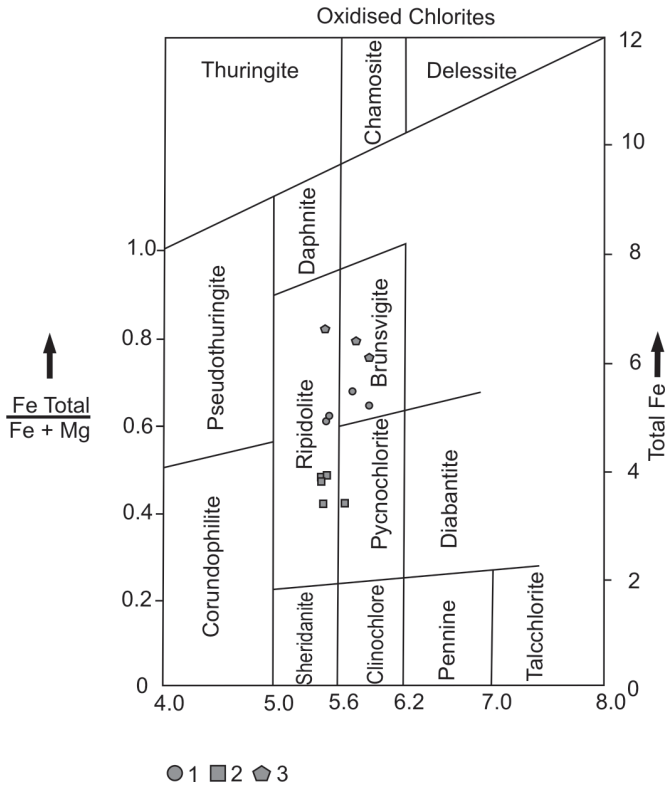

Fig. 5. Classification diagram for analysed chlorites [10]

1 – chlorites from mica-chlorite lamines (#mg = 0.319÷0.418), 2 – chlorites from mica-chlorite lamines (#mg = 0.526÷0.589), 3 – chlorites from garnet porphyroblasts (#mg = 0.203÷0.263)

According to previous conclusions we can assume that chlorites in investigated rocks are ortochlorites from the diabantite-piknochlorite-ripidolite group. This conclusion seems to be confirmed by the fact, that ripidolite (most chemical analyses are placed in the ripidolite area in Hey's diagram) is a product of biotite alternation [5] and this process is common in investigated exotic schist cobbles.

Feldspars

Plagioclases, often forming porphyroblasts (Fig. 3F), are relatively rare in investigated rocks and reach up to a few vol. % (most often not more than 1.3 vol. %. (Tab. 1). They occur in quartz laminae and also in white mica-chlorite laminae. They are up to 1 mm, non-twinned, with inclusions of different minerals (most often white mica). The results of chemical analysis were plotted on classification diagram (Fig. 6). Plagioclases in analyzed rocks are albite (Ab_{91-92}) and oligoclase (Ab_{84-85}). In CL analyses they have green-yellow colors, which is most probably a result of the occurrence of MnO [6]. These colors have extremely low intensity, because in studied feldspars a very low amount of MnO (up to 0.13 wt. %) was identified.

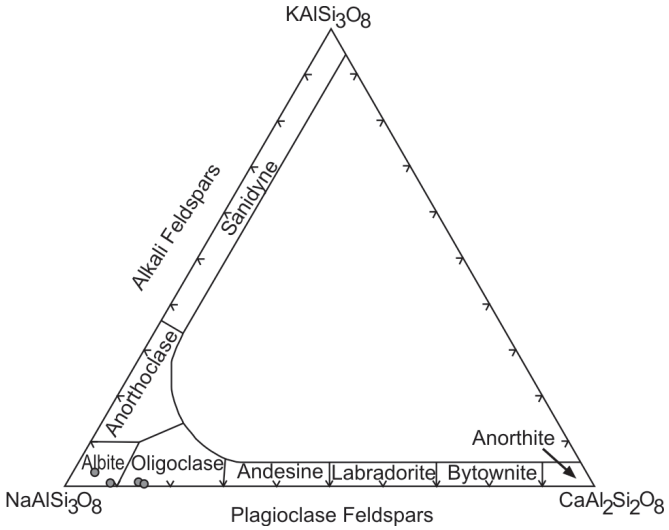

Fig. 6. Feldspar classification diagram

Garnets

Garnets are quite often noticed in investigated rocks (Tab. 1). Garnet's porphyroblasts range from 0.2÷0.9 vol. %, up to 4.4÷8.7 vol. %. They are fractured, with chlorite or mica filling veinlets. In studied minerals, characteristic inclusions of quartz occurred. Garnet's porphyroblasts reach about 2 to 5 mm and have various shapes (spherical, ellipsoidal and tectonically elongated) (Fig. 3D, E). The smaller porphyroblasts occur within mica-chlorite laminae, while the larger occur both in mica-chlorite and in quartz laminae. The results of SEM-EDS analysis (Tab. 2) also proved that investigated garnets are almandines ($Alm_{58.50-79.58}$). SEM-EDS analysis (mapping) was also very useful to suggest zonation in investigated garnets. In the cores a higher amount of FeO (34.07÷35.69 wt. %) and a lower amount of CaO (1.96÷3.07 wt. %) were measured, while in the rims the amount of FeO decreases (24.48÷32.25 wt. %) and the amount of CaO increases (6.30÷9.63 wt. %). As a result of this situation there are different almandine and grossular end-members contents calculated (core – $Alm_{75.55-79.58}Gro_{4.83-8.09}Py_{6.30-9.48}Sp_{5.05-9.31}$; rim – $Alm_{58.50-70.58}Gro_{17.22-25.67}Py_{4.50-9.48}Sp_{1.40-15.88}$). The amount of pyrope end-member is quite similar in rims and cores and

Table 2. Garnet SEM-EDS analysis

	RIM								CORE									
	A1-2a	A1-7a	A1-8b	A2-3a	A2-4a	B1.1-5c	B1.4-2a	B1.4-4a	A1-2b	A1-2c	A1-7b	A1-7c	A1-8a	A2-3b	A2-4b	B1.1-5a	B1.4-2b	B1.4-4b
SiO_2	36.69	36.98	37.05	36.88	36.11	36.90	36.66	37.03	36.32	36.19	36.28	37.26	36.45	36.60	37.19	36.83	36.17	36.69
TiO_2	-	-	-	-	0.09	0.07	0.05	0.01	-	-	-	-	-	-	0.04	0.04	0.08	0.06
Al_2O_3	20.96	21.14	21.60	21.16	20.78	20.97	20.67	21.34	20.79	20.81	20.98	21.36	21.27	21.16	21.37	21.03	21.05	20.99
Cr_2O_3	-	-	-	0.04	0.66	0.06	0.09	0.04	0.05	0.20	-	-	-	0.04	0.14	0.18	-	0.06
FeO	32.02	32.25	31.63	31.35	27.85	30.15	27.50	31.11	35.69	34.07	36.03	29.61	35.09	30.36	30.6	26.48	29.11	32.01
MnO	0.62	0.73	0.82	1.01	3.41	2.47	6.50	1.69	2.83	4.09	2.23	1.63	2.68	1.97	2.15	7.02	4.95	1.86
MgO	1.55	2.06	1.91	2.33	1.47	1.93	1.41	2.09	2.37	1.57	2.24	1.13	2.07	1.77	1.9	1.39	1.66	2.02
CaO	8.17	6.84	6.99	7.23	9.63	7.45	7.12	6.70	1.96	3.07	2.24	9.00	2.43	8.11	6.62	7.04	6.97	6.30
Total	100%	100%	100%	100%	100%	100%	100%	100%	100%	100%	100%	100%	100%	100%	100%	100%	100%	100%
Cations basing on 24 O atoms in the formula																		
Si	5.918	5.944	5.937	5.920	5.834	5.935	5.933	5.941	5.916	5.908	5.907	5.971	5.918	5.894	5.962	5.940	5.859	5.919
Al^{IV}	0.082	0.056	0.063	0.080	0.166	0.065	0.067	0.059	0.084	0.092	0.093	0.029	0.082	0.106	0.038	0.060	0.141	0.081
	6.000	6.000	6.000	6.000	6.000	6.000	6.000	6.000	6.000	6.000	6.000	6.000	6.000	6.000	6.000	6.000	6.000	6.000
Al^{VI}	3.902	3.948	4.017	3.923	3.790	3.910	3.876	3.977	3.908	3.913	3.933	4.006	3.988	3.910	3.999	3.938	3.878	3.910
Cr	-	-	-	0.005	0.084	0.008	0.012	0.005	0.006	0.025	-	-	-	0.005	0.017	0.023	-	0.008
Fe^{3+}	0.098	0.052	-	0.072	0.116	0.074	0.106	0.017	0.086	0.062	0.067	-	0.012	0.085	-	0.035	0.112	0.074
Ti	-	-	-	-	0.010	0.008	0.006	0.001	-	-	-	-	-	-	0.005	0.004	0.010	0.008
	4.000	4.000	4.017	4.000	4.000	4.000	4.000	4.000	4.000	4.000	4.000	4.006	4.000	4.000	4.021	4.000	4.000	4.000
Mg	0.373	0.493	0.457	0.557	0.355	0.464	0.340	0.499	0.577	0.383	0.544	0.270	0.502	0.424	0.453	0.333	0.400	0.487
Fe^{2+}	4.221	4.284	4.239	4.137	3.597	3.982	3.617	4.157	4.776	4.591	4.839	3.968	4.753	4.004	4.102	3.537	3.832	4.244
Mn	0.085	0.100	0.111	0.138	0.467	0.337	0.891	0.229	0.39	0.566	0.307	0.222	0.369	0.268	0.292	0.96	0.679	0.254
Ca	1.411	1.177	1.199	1.244	1.666	1.284	1.235	1.152	0.342	0.537	0.391	1.545	0.423	1.400	1.136	1.216	1.210	1.088
	6.09	6.054	6.006	6.076	6.085	6.067	6.083	6.037	6.085	6.077	6.081	6.005	6.047	6.096	5.983	6.046	6.121	6.073
Almandine	69.31	70.76	70.58	68.09	59.11	65.63	59.46	68.86	78.49	75.55	79.58	66.08	78.60	65.68	68.56	58.5	62.6	69.88
Andradite	2.45	1.30	0.00	1.80	2.90	1.85	2.65	0.43	2.15	1.55	1.68	0.00	0.30	2.13	0,00	0.88	2.80	1.85
Grossular	22.33	19.00	19.96	19.82	25.67	20.47	19.29	18.9	4.83	8.09	5.86	25.73	6.89	22.19	18.85	19.62	18.8	17.22
Pyrope	6.12	8.14	7.61	9.17	5.83	7.65	5.59	8.27	9.48	6.30	8.95	4.50	8.30	6.96	7.57	5.51	6.53	8.02
Spessartine	1.40	1.65	1.85	2.27	7.67	5.55	14.65	3.79	6.41	9.31	5.05	3.70	6.10	4.40	4.88	15.88	11.09	4.18
Uvarovite	-	-	-	0.13	2.10	0.20	0.30	0.13	0.15	0.63	-	-	-	0.13	0.42	0.58	-	0.20
Total	101.61	100.85	100.00	101.28	103.28	101.35	101.94	100.38	101.51	101.43	101.12	100.01	100.19	101.49	100.28	100.97	101.82	101.35

Table 3. Results of tourmaline SEM-EDS analysis

	COLOURLESS ZONES INTENSE BROWN LIGHT BROWN								BLUE ZONES					BROWN ZONES				
	A1-5a	A1-5e	A1-6c	A2-2b	A4-1a	A4-1c	B1.1-1b	B1.1-3c	A1-5b	A1-5c	A1-5d	A1-6a	A1-6b	A2-2a	A4-1b	B1.1-1a	B1.1-3a	B1.1-3b
SiO_2	42.73	42.37	42.80	42.72	42.22	43.22	43.32	43.28	42.22	41.96	42.36	42.35	42.49	39.51	40.45	42.13	40.89	40.53
TiO_2	0.85	0.88	0.91	0.81	0.97	0.81	0.97	0.77	1.41	1.05	1.06	0.74	0.97	1.55	0.61	0.51	1.91	2.55
V_2O_5	-	-	-	-	0.05	0.01	0.03	0.01	-	-	-	-	-	-	0.08	0.19	0.11	0.07
Al_2O_3	37.77	38.13	37.40	36.75	37.68	36.78	35.8	36.15	35.20	35.89	35.30	35.94	35.67	33.56	39.44	33.16	30.22	29.39
Cr_2O_3	-	-	-	-	0.02	0.14	0.07	0.09	-	-	-	-	-	0.57	0.13	0.14	0.08	0.28
FeO	8.06	7.70	8.11	8.51	8.54	8.96	8.59	8.99	11.70	10.88	10.76	11.47	10.47	21.59	15.06	13.69	15.29	15.40
MgO	7.58	7.87	7.85	8.00	7.54	7.61	8.43	7.95	6.64	7.29	7.43	6.66	7.09	0.35	2.18	6.73	7.33	7.26
CaO	0.90	0.85	0.85	1.23	0.99	0.12	0.24	0.37	0.23	0.50	0.44	0.09	0.44	0.06	0.14	0.87	2.55	2.74
MnO	0.11	0.05	-	0.01	0.04	-	-	0.02	-	-	0.02	0.12	0.14	0.15	0.04	0.04	0.17	0.07
K_2O	0.07	0.07	0.08	0.03	0.06	0.03	0.03	0.07	0.05	0.06	0.06	0.04	0.07	0.12	0.06	0.07	0.01	0.07
Na_2O	1.92	2.08	1.99	1.93	1.82	2.23	2.53	2.30	2.55	2.38	2.56	2.57	2.66	2.53	1.80	2.48	1.43	1.64
Total	100%	100%	100%	100%	100%	100%	100%	100%	100%	100%	100%	100%	100%	100%	100%	100%	100%	100%
Cations basing on 24.5 O atoms in the formula																		
Si	5.995	5.942	6.007	6.017	5.944	6.081	6.098	6.098	6.039	5.980	6.040	6.044	6.049	5.949	5.838	6.105	6.020	5.993
B	3.000	3.000	3.000	3.000	3.000	3.000	3.000	3.000	3.000	3.000	3.000	3.000	3.000	3.000	3.000	3.000	3.000	3.000
Al	6.000	6.000	6.000	6.000	6.000	6.000	5.939	6.000	5.934	6.000	5.929	6.000	5.985	5.957	6.000	5.662	5.243	5.121
Fe^{3+}	-	-	-	-	-	-	0.061	-	0.066	-	0.071	-	0.015	0.043	-	0.338	0.757	0.879
	6.000	6.000	6.000	6.000	6.000	6.000	6.000	6.000	6.000	6.000	6.000	6.000	6.000	6.000	6.000	6.000	6.000	6.000
Al	0.245	0.301	0.186	0.100	0.252	0.098	-	0.002	-	0.029	-	0.044	-	-	0.710	-	-	-
Fe^{2+}	0.946	0.904	0.950	1.002	1.004	1.055	0.950	1.060	1.335	1.298	1.212	1.369	1.232	2.675	1.817	1.320	1.126	1.026
Mg	1.587	1.646	1.643	1.680	1.582	1.597	1.768	1.670	1.416	1.548	1.580	1.418	1.507	0.078	0.470	1.452	1.609	1.601
Ti	0.091	0.093	0.096	0.086	0.103	0.086	0.103	0.083	0.152	0.113	0.115	0.081	0.103	0.176	0.066	0.056	0.211	0.284
Mn	0.013	0.005	-	0.002	0.005	-	-	0.002	-	-	0.002	0.015	0.017	0.020	0.005	0.005	0.022	0.009
	2.881	2.948	2.875	2.871	2.946	2.836	2.821	2.818	2.902	2.988	2.910	2.926	2.859	2.949	3.068	2.833	2.968	2.921
Na	0.524	0.566	0.541	0.527	0.497	0.608	0.690	0.627	0.705	0.656	0.708	0.710	0.735	0.739	0.502	0.695	0.409	0.470
Ca	0.135	0.127	0.130	0.186	0.149	0.020	0.037	0.056	0.034	0.076	0.066	0.015	0.066	0.009	0.022	0.135	0.401	0.434
K	0.013	0.013	0.015	0.005	0.009	0.002	0.005	0.013	0.009	0.013	0.013	0.007	0.013	0.022	0.013	0.013	0.002	0.015
[ ]	0.329	0.295	0.314	0.282	0.344	0.371	0.268	0.304	0.251	0.255	0.213	0.268	0.186	0.230	0.463	0.157	0.187	0.081
	1.000	1.000	1.000	1.000	1.000	1.000	1.000	1.000	1.000	1.000	1.000	1.000	1.000	1.000	1.000	1.000	1.000	1.000

reaches 4.50÷9.48 wt. %. The amount of spessartite end-member also does not change noticeably from core to rim, although sometimes the higher contents, up to 15.88 wt. % are measured in the rims. All changes of chemical composition are only noticed in spherical and ellipsoidal garnet porphyroblasts, while in those tectonically elongated no such changes were detected (probably) due to homogenization process during tectonic movements.

Tourmaline

In investigated rocks, tourmaline forms columns and reaches up to 2.5 vol. %. They occur in both mica-chlorite and quartz layers. Characteristic brown and blue zones are often noticed in thin sections (Fig. 3G, H). The results of SEM-EDS analysis (Tab. 3) classify those minerals as alkali tourmalines (Fig. 7). Measured values of Mg, Fe, Na and a vacancy in X position classify analyzed tourmalines within the alkali group as dravites (Fig. 8). Only two analyses were plotted in the tourmalines classification diagram in schorl field. These two analyses were made from very intense brown zones, where the contents of FeO were the highest (15.06÷21.59 wt. %). Those brown parts may be relicts of tourmalines (schorl) that occurred in primary pelitic-

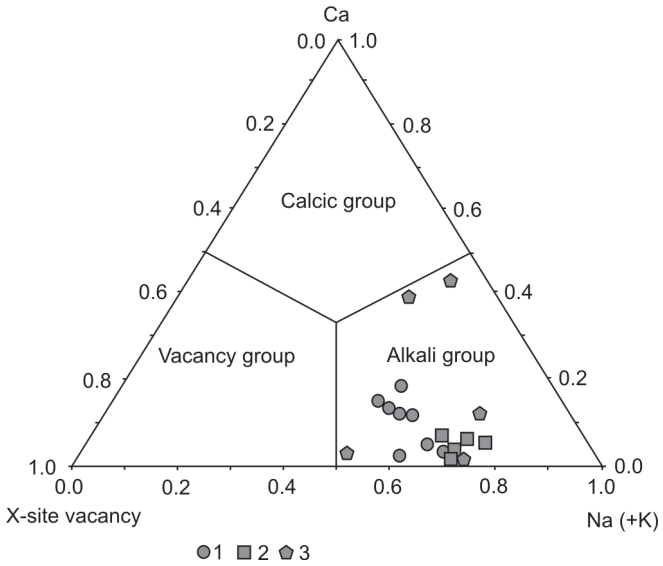

Fig. 7. Classification diagram of tourmaline groups [8]

Analysis were taken from: 1 – colourless zones, 2 – blue zones, 3 – brown zones

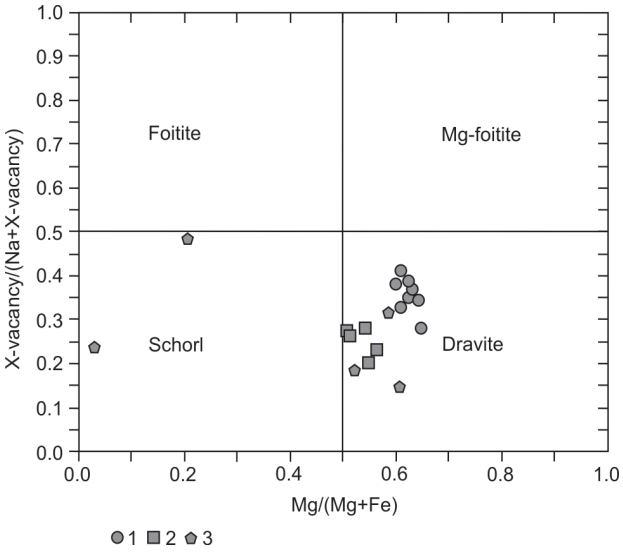

Fig. 8 Mg/(Mg+Fe) vs. X-vacancy/(Na + X-vacancy) diagram for analyzed tourmalines

Analysis were taken from: 1 – colourless zones, 2 – blue zones, 3 – brown zones

mudstone protolith rocks as heavy minerals and during metamorphism were overbuilt by dravite.

Accessory minerals

Accessory minerals like apatite, zircon, rutile, ilmenite are also present in investigated rocks.

Apatites are quite common (0.3÷1.8 vol. %) (Tab. 1) in both mica-chlorite and quartz layers. They are small (up to 0.1 mm) and oval. In CL analysis they have green colour, which is a result of the occurrence of REE (detected during SEM-EDS analysis – Y_2O_3 up to 2.46 wt. %, Nb_2O_5 up to 2.47 wt. %). Zones with a different intense green color can be noticed. This phenomenon is probably related to changes of REE contents in apatite blasts.

Ilmenite and Ti oxides occur often in investigated rocks, although they do not reach more than 1.5 vol. % (Tab. 1).

Calcite

Calcite (up to 3.2 vol. %) forming thin veins (about 1÷2 cm long and 0.1 mm thick) is also noticed in investigated rocks. Larger veins crossing whole samples were also detected (1÷2 mm thick). In CL analysis calcite veins have colors from yellow to dark-red, which is a result of MnO occurrence.

Discussion

Protolith

The SEM-EDS analysis data of tourmalines was very useful to determine the protolith of investigated exotic schist cobbles. The results of chemical analyses were plotted on Al-Fe(tot)-Mg (Fig. 9) and Ca-Fe(tot)-Mg (Fig. 10) diagrams, which show the typical chemical composition of tourmalines from different rock types.

In the Al-Fe(tot)-Mg [9] diagram (Fig. 9) most points representing chemical analyses from colorless zones in tourmalines, are plotted in "metapelites and metapsammites not

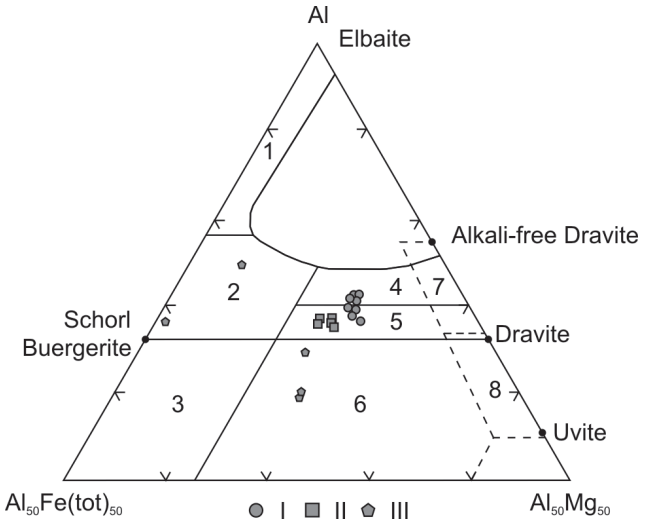

Fig. 9. Al-Fe(tot)-Mg (molecular proportions) diagram [9]

Analyses were taken from: I – colorless zones, II – blue zones, III – brown zones. 1 – Li-rich granitoid and their associated pegmatites and aplites, 2 – Li-poor granitoids and their associated pegmatites and aplites, 3 – Fe^{3+} – rich quartz-tourmaline rocks, 4 – metapelites and metapsammites coexisting with an Al-saturating phase, 5 – metapelites and metapsammites not coexisting with an Al-saturating phase, 6 – Fe^{3+} – rich quartz-tourmaline rocks, calc-silicate rocks and metapelites, 7 – low-Ca metaultramafics and Cr, V-rich metasediments, 8 – metacarbonates and meta-pyroxenites

coexisting with an Al-saturating phase" field. Points representing analyses from blue zones and a few from colorless zones are plotted in "metapelites and metapsammites coexisting with an Al-saturating phase" field, while points representing analyses from brown zones are plotted in "Fe^{3+} rich quartz-tourmaline rocks, calc-silicate rocks and metapelites". Only two analyses, due to a higher amount of Fe in extremely intense brown zones (probably relic of heavy minerals) are plotted in "Li-poor granitoids and their associated pegmatites and aplites" field. A similar situation can be noticed in the Ca-Fe(tot)-Mg (Fig. 10) diagram, where most points are plotted in "Ca-poor metapelites, metapsammites and quartz-tourmaline rocks" field.

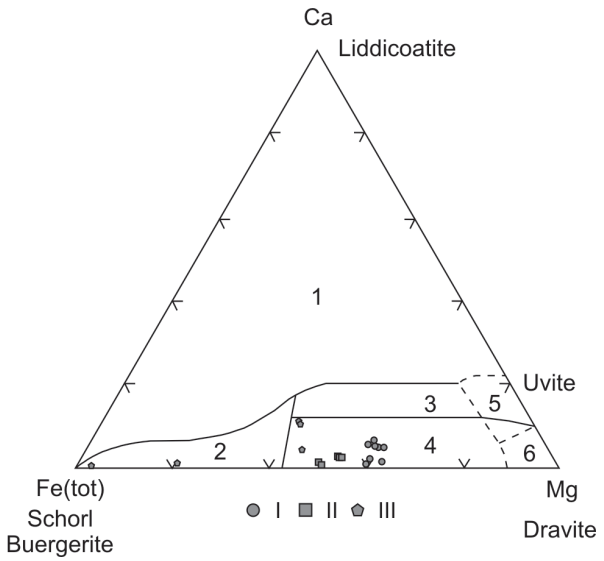

Fig. 10. Ca-Fe(tot)-Mg (molecular proportions) diagram [9]

Analyses were taken from: I – colourless zones, II – blue zones, III – brown zones. 1 – Li-rich granitoid pegmatites and aplites, 2 – Li-poor granitoid pegmatites and aplites, 3 – Ca-rich metapelites, metapsammites and calc-silicate rocks, 4 – Ca-poor metapelites, metapsammites and quartz-tourmaline rocks, 5 – metacarbonates, 6 – meta-ultramafics

On the basis of the tourmaline SEM-EDS analysis and microscopic observations, it is possible to state that most likely, the protolith of investigated rock cobbles were pelitic-mudstone rocks. This conclusion seems to be confirmed by the fact that pelitic-mudstone rocks have the ability to accumulate boron, essential to tourmaline crystallization [5].

Metamorphic conditions

Metamorphic transformation of investigated rocks formed during two stages.

In the first stage the protolith had been regionally, progressively metamorphosed in conditions of lower temperatures of almandine-amphibolite facies or in higher temperatures of green schist facies. It is difficult to obtain PT conditions more precisely, because both biotite and almandine may be present in the highest temperatures of green schist facies. In such conditions, plagioclases with more than 7% anortite (as albite and oligoclase in studied rocks) may also be stable. It seems to be right though, that the most likely conditions of this stage of metamorphism were those of low-temperature almandine-amphibolite facies. The occurrence in investigated schist cobbles quartz + muscovite + biotite + almandine + plagioclase paragenesis (which is characteristic for pelitic-mudstone rocks metamorphosed in epidote-amphibolite facies according to Winkler [26]) can confirm this conclusion. The results of SEM-EDS analysis of garnets plotted on Miyashiro & Kuculu diagram (Fig. 11) (Miyashiro and Kuculu in: [1]) also seem to confirm such an interpretation (all points that were plotted on the diagram represents garnets form epidote-amphibolite facies).

The second stage is represented by retrogressive metamorphism, related to tectonic activity (faults, shear zones). It can be stated on the basis of the occurrence in investigated rocks of garnet porphyroblasts with elongated shape due to tectonic processes. Moreover, the occurrence of phengite, albite and secondary chlorite (after biotite) is characteristic

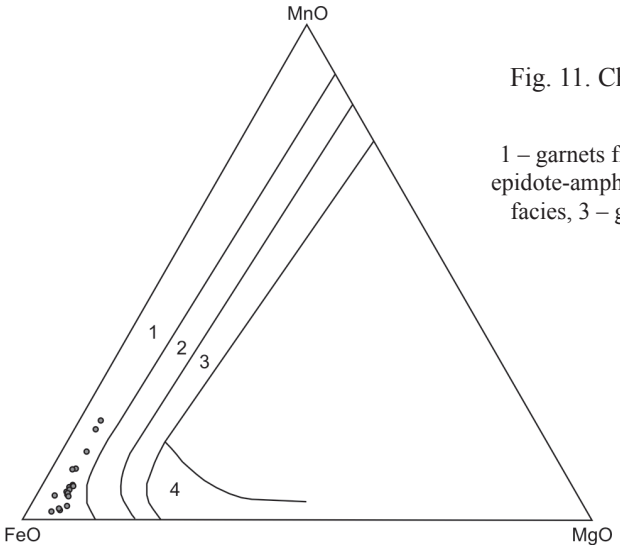

Fig. 11. Chemical composition of garnets. Individual fields represent various metamorphic zones

1 – garnets from greenschists and epidote-amphibolite facies, 2 – garnets from epidote-amphibolite facies and low-temperature subfacies of garnet-amphibolite facies, 3 – garnets from amphibolite facies, 4 – garnets from granulite facies (according to Miyashiro and Kuculu in [1])

for this type of metamorphism. The changes in PT conditions were also recorded in zones of garnet porphyroblasts. The increasing almandine and pirope end-members and decreasing grossular, andradite and spessartite end-members from core to rim can be a sign of a progressive metamorphism [2]. In a case of garnet porphyroblasts in investigated rocks, the increasing grossular and spessartite end members and decreasing almandine end member form core to rim are noticed. Therefore, cores seem to be a relict of the progressive stage of metamorphism (almandine-amphibolite facies of regional metamorphism) while rims overbuilt cores during high-P metamorphism. The tectonically elongated garnet porphyroblasts do not show zones of different chemical compositions. It is a result of their transformation and homogenization during intense deformation movements in shear zones.

Source of exotic cobbles

It is quite reasonable that investigated exotic schist cobbles from Krosno beds are related to thick-bedded, middle- to coarse-grained, polymictic Otryt sandstones [3]. In those sandstones grains of schists as well as different crystalline rocks (with quartz, alkaline feldspars, plagioclases, muscovite and biotite), quartzite and limestone are present [7]. It means that the composition of these sandstones is very similar to exotic rock cobbles from the investigated area, which leads to the conclusion that source area and transport directions (from SE) must have been the same for both Otryt sandstones and analyzed exotic schist cobbles. Such a direction has been determined [19] on the basis of the occurrence in Otryt sandstones characteristic oriented structures. According to Ślączka and Wieser [19], the source area of these exotic rock cobbles was small islands situated between the Dukla and Silesian subbasins and being the north-western extension of the Marmarosh or Rakhiv massifs. These islands were composed of crystalline rocks and in some parts of Eocene-Oligocene limestones [3].

Conclusions

Investigated exotic schist cobbles are grey and green in color, with mica-chlorite and quartz layers most often reaching up to 0.5 mm. Some of these rocks are tectonically deformed and show S-C structures (mica fish).

The cobbles consist of: quartz, white mica (phengite) and chlorite (ripidolite). The other minerals like garnets ($Alm_{58-79}Gro_{4-25}Py_{4-9}$), tourmalines (dravite), biotite (most often altered) and plagioclases (albite, oligoclase) are also present as well as apatite, zircon, Ti oxides and ilmenite. Small or larger calcite veins are also common.

The protolith of investigated schists was pelitic-mudstone rocks (such a conclusion was made according to Henry and Guidotti's [9] diagrams based on chemical composition of tourmalines).

Primary protolith rocks were metamorphosed in conditions of epidote-amphibolite facies (quartz + white mica + biotite + plagioclase + almandine paragenesis) [26]. The next stage was retrogressive, high-pressure metamorphism related to tectonic activity.

The rims of garnet porphyroblasts, elongated and homogenized garnet blasts, the occurrence of phengite and secondary chlorite and the s-c structures (mica fish) are evidences of the retrogressive metamorphism.

The transport of the clastic material (with exotic rock cobbles) of Krosno Beds was from SE. The source area was probably the islands which were the north-western extension of Marmarosh or Rakhiv massifs, situated between the Dukla and Silesian subbasins [19].

Please cite as: Nafta-Gaz 2014, no. 10, pp. 659–670

This paper is based on author's master thesis: Mineralogical and petrological investigation of exotic schists with garnets from Krosno Beds, Silesian Unit, Bieszczady Mts.

References

[1] Antipin V.: *Petrology, geochemistry of granitoids of various facies*. Nauka 1977, 158 pp.

[2] Azor A., Simancas J., Exposito I., Lodeiro F., Poyatos D.: *Deformation of garnets in a low-grade shear zone*. Journal of Structural Geology 1977, 19 (9), pp. 1137–1148.

[3] Bak K., Rubinkiewicz J., Garecka M., Machaniec E., Dziubinska B.: *Exotics-bearing layer in the oligocene flysh of the Krosno beds in the Fore-Dukla Zone (Silesian Nappe, Outer Carpathians), Poland*. Geologica Carpathica 2001, 52 (3), pp. 159–171.

[4] Bieda F.: *Seventh level of large foraminifera in Polish Outer Carpathians*. Rocznik Polskiego Towarzystwa Geologicznego 1963, 33 (2), pp. 189–218.

[5] Borkowska M., Smulikowski K.: *Rock forming minerals*. Wydawnictwo Geologiczne, Warszawa 1973, 447 pp.

[6] Goetze J., Krbetschek M. R, Habermann D., Wolf D.: *High-resolution cathodoluminescence of feldspar minerals*. [in:] Pagel M., Barbin V., Blanc P., Ohnenstetter D (eds.) Cathodoluminescence in Geosciences. Springer 2000, 514 pp.

[7] Haczewski G., Bak K., Kukulak J.: *Commentary to detailed geological map of Poland 1:50 000; Dzwiniacz Gorny sheet: 1069*. Państwowy Instytut Geologiczny, Warszawa 1997.

[8] Hawthorne F., Henry D.: *Classification of the minerals of the tourmaline group*. European Journal of Mineralogy 1999, 11 (2), pp. 201–215.

[9] Henry D., Guidotti C.: *Tourmaline as petrogenetic indicator mineral: an example from the staurolite-grade metapelites of NW Maine*. American Mineralogist 1985, 70, pp. 1–15.

[10] Hey M.: *A new review of the chlorites*. Mineralogical Magazine 1954, 30, pp. 277–292.

[11] Ivan P., Sykora M., Demko R.: *Blueschists in the Cretaceous exotic conglomerates of the Klape Unit (Pieniny Klippen Belt, Western Carpathians): their genetic types and implications for source area*. Geologia 2006, 32 (1), pp. 47–63.

[12] Kusmierek J., Tokarski A.: *The frontal linge of the Iwonicz recumbent fold in Bieszczady Mts. Group*. Nafta 1965, 21 (11), pp. 317–321.

[13] Matyasik I.: *Petroleum System of Silesian and Dukla Units in Jaslo–Krosno–Sanok area*. Nafta-Gaz 2009, no. 3, pp. 201–206.

[14] Mochnacka K., Tokarski A.: *New location with exotic-bearing layers within Krosno Beds near*. Ustrzyki Górne. Rocznik Polskiego Towarzystwa Geologicznego 1972, 42 (2–3), pp. 229–238.

[15] Olszewska B.: *Oligocene Foraminifera from Roztoki Dolne with its paleoecological interpretation*. Sprawozdanie z Posiedzeń Komisji Nauk Geologicznych PAN, Oddział w Krakowie 1977, 21 (1), pp. 222–223.

[16] Oszczypko N., Oszczypko-Clowes M., Salata D.: *Exotic rocks of the Krynica Zone (Magura nappe) and their paleogeographic significance*. Geologia 2006, 32 (1), pp. 21–45.

[17] Probulski J., Dudek L., Sowizdzal K.: *Validation of geological cross sections' interpretation from Polish part of Carpathians by means of restoration of sedimentary basin development*. Nafta-Gaz 2009, no. 12, pp. 929–933.

[18] Rubinkiewicz J.: *Tectonics of the Dukla overthrust's zone in western part of the Bieszczady Mts*. Przegląd Geologiczny 1996, 44 (12), pp. 1199–1204.

[19] Slaczka A., Wieser T.: *Shales bearing exotic rocks from Krosno Beds near Baligrod*. Kwartalnik Geologiczny 1962, 6, pp. 662–667.

[20] Slaczka A.: *Genesis of exotic-bearing layer from Bukowiec near Uzocka Pass*. Rocznik Polskiego Towarzystwa Geologicznego 1961, 31 (1), pp. 129–143.

[21] Slaczka A.: *Lower Krosno Beds from Roztoki Dolne*. Rocznik Polskiego Towarzystwa Geologicznego 1963, 33 (2), pp. 181–186.

[22] Slaczka A.: *Preliminary results of the Wetlina IG-2 borehole in the Bieszczady Mts*. Kwartalnik Geologiczny1969, 13 (3), pp. 712–713.

[23] Slaczka A.: *The geology of the Dukla unit – Polish Flysch Carpathians*. Prace Instytutu Geologicznego 1971, 63, pp. 1–167.

[24] Swidzinski H.: *Outer Carpathians between Dunajec and San*. Regionalna Geologia Polski 1953, 1 (2), pp. 362–422.

[25] Tokarski A.: *Geology and geomorphology of the Ustrzycki Górne area (Polish Eastern Carpathians)*. Studia Geologica Polonica 1975, 48, pp. 7–90.

[26] Winkler H. G. F.: *Petrogenesis of metamorphic rocks*. 2nd edn. Springer New York 1967, 334 pp.

Mgr Konrad ZIEMIANIN
Asystent w Zakładzie Geologii i Geochemii.
Instytut Nafty i Gazu – Państwowy Instytut Badawczy
ul. Lubicz 25A
31-503 Kraków
E-mail: *ziemianin@inig.pl*

Dr Anna WOLSKA
Starszy wykładowca w Instytucie Nauk Geologicznych
Uniwersytet Jagielloński
ul. Oleandry 2a
30-061 Kraków
E-mail: *a.wolska@uj.edu.pl*